Available online at www.sciencedirect.com

ScienceDirect

Procedia Engineering 10 (2011) 2755–2767

Engineering Procedia

ICM11

# Fatigue life prediction of notched components: a comparison between the theory of critical distance and the classical stress-gradient approach

Andrea Spaggiari [a]*, Davide Castagnetti[a], Eugenio Dragoni[a], Simone Bulleri[b]

[a]*University of Modena and Reggio Emilia, via Amendola, 2 Campus S. Lazzaro, 42122 RE, Italy*
[b]*Galtech S.r.l. Via Kennedy 10 - 42124 Reggio Emilia, Italy*

**Abstract**

Fatigue life prediction for machine components is a key factor in the industrial world and several methods can be traced in technical literature to estimate life of notched components. The paper correlates the classical stress-gradient approach, here after called support factor (SF) method, proposed by Siebel, Neuber and Petersen with the modern theory of critical distance (TCD) approach by Tanaka and Taylor. On the one hand, the main asset of the SF method is that it relies only on the knowledge of the maximum stress and stress gradient in the hot spot. By contrast, the TCD needs the calculation of the stress distribution for a finite depth inside the material. On the other hand, the main drawback of the SF method is that the material parameter $\rho^*$ is available only for a limited collection of materials and moreover the experimental procedure to retrieve this parameter is not clearly defined in the technical literature. In order to overcome this limitation, the paper investigates the correlation between the material parameter $\rho^*$ and the critical distance $L$ of the TCD by relying on a specific stress function. A comparison between the SF method and the TCD is then performed by considering three different benchmark geometries: a general V-notch in a plate, a pressure vessel and an industrial oleo-hydraulic distributor. Effective stresses are analytically retrieved and compared using both methods for the first two benchmarks and with the help of an elastic finite element analysis for the last one. The resus appear good in terms of fatigue life prediction, especially for the industrial case study.



*Keywords*: notched components; fatigue; critical distance; material parameter

**Nomenclature**

| | | | |
|---|---|---|---|
| $a$ | Hole radius | $R_s$ | Yield strength |
| $A$ | First constant of the homographic function | $s_\sigma$ | Normalized stress gradient |
| $B$ | Second constant of the homographic function | $S'_N$ | Fatigue limit for smooth specimens |
| $C$ | Third constant of the homographic function | $x$ | Linear coordinate |
| $E$ | Young's Modulus | $\Delta K_{th}$ | Threshold stress intensity factor |
| $G_\sigma$ | Stress gradient at the hot spot | $\beta$ | Opening angle |
| $L$ | Taylor's critical distance | | |

1877-7058 © 2011 Published by Elsevier Ltd. Open access under CC BY-NC-ND license.
Selection and peer-review under responsibility of ICM11 doi:10.1016/j.proeng.2011.04.459

| | | | |
|---|---|---|---|
| $k$ | Parameter of the stress function | $v_d$ | Support factor |
| $K_f$ | Fatigue notch factor | $\theta$ | Polar coordinate |
| $K_t$ | Stress concentration factor | $\rho$ | Notch radius |
| $n$ | Exponent of the Basquin equation | $\rho^*$ | Siebel material parameter |
| $N^S$ | Cycles to failure according to SF method | $\sigma_a$ | Fatigue strength in Basquin equation |
| $N^T$ | Cycles to failure according to Taylor's method | $\sigma_f$ | Maximum stress in Basquin equation |
| $q$ | Notch sensitivity | $\sigma_{eff}^S$ | SF effective stress |
| $p$ | Parameter used in elastic analysis [19] | $\sigma_{eff}^T$ | TCD effective stress |
| $r$ | Radial coordinate of the pressure vessel | $\sigma_{\max}$ | Maximum principal stress |
| $r_0$ | Notch tip radius | | |
| $r_e$ | Outer radius of the pressure vessel | | |
| $r_i$ | Inner radius of the pressure vessel | | |
| $R$ | Fatigue ratio | | |
| $R_m$ | Maximum tensile strength | | |

## 1. Introduction

The work deals with a comparison between two fatigue life prediction theories: the recent Theory of Critical Distance (TCD) from Tanaka [1] and Taylor [2]-[6] and the classic local stress-gradient approach from Peterson [7], Siebel and Steiler [8] and Neuber [9], hereafter called support factor method (SF). Since the earlier works on fatigue in the middle of the 19th century, several methods for fatigue life prediction have been proposed. Two parameters can be used in the classic approach to fatigue in mechanical components: the first one called stress concentration factor ($K_t$) takes into account the effect of the notch geometry on the stress field. The second one, called notch sensitivity ($q$) measures how sensitive a material is to notches or geometric discontinuities. These two parameters are combined in order to obtain the fatigue notch factor, ($K_f$), widely used and tabulated in technical literature [10]

$$K_f = 1 + q(K_t - 1) \tag{1}$$

Unfortunately, this simple approach cannot be applied to notched components of many real applications due to their complex geometry which prevents the calculation of a nominal stress and consequently the stress intensity factor ($K_t$).

A number of different approaches have been proposed to solve this problem. Most of them rely on the idea that the stress level must be high enough, not only at the hot spot, but also for some distance around the hot spot [3] in order to produce fatigue failure. Initially proposed by [7]-[9], this approach (called "process zone" method) is based on a support factor $v_d$ and has the peculiarity that the fatigue limit prediction relies on elastic analyses. In particular, an effective stress is calculated by combining the stress gradient at the hot spot with the support factor which depends on a characteristic length $\rho^*$. This parameter is a property of the material and is often found through empirical laws linked to the mechanical, tensile properties and microstructure of the material. The support factor is also defined as $K_t / K_f$ the ratio between the fatigue limit in presence of stress gradient and the fatigue limit without gradients [11], thus being always greater than one. Other formulas were proposed by Bollenrath [13] and Troost [14]

that start from the plasticization of the material around the notch and elaborate expressions for the support factor. Eichlseder [15]-[16] and Reggiani [11] proposed refined formulas for the support factor which start from FE analysis data. The limit of this method is that the characteristic length $\rho^*$ is hard to find in technical literature and available only for some specific classes of material [17].

More recently Tanaka [1] and Taylor [2]-[6] independently proposed the TCD, which again belongs to the category of "process zone" methods. The stress distribution originated by the notch is investigated by applying the linear elastic fracture mechanics (LEFM) in order to find the stress life prediction. Hence, through the LEFM, the method can efficiently deal with stress concentrations or singularities originated by the notches, but still needs a parameter to address the sensitivity of the material to the notches. This parameter, called critical distance *L*, can be calculated using El Haddad's equation [18] and is used to find the effective stress in the component on the basis of the stress field which is mainly retrieved from FE analyses. The parameters needed to define the critical distance, in particular the threshold stress intensity factor [18], can be retrieved from simple experimental tests on a notched compact tension (CT) specimen. In technical literature, the critical distance for a large class of engineering materials is currently available [6]. The TCD is a quite general approach and eliminates the uncertainty of the previous methods. The application of the TCD to different components [2]-[6] compared to experimental tests, has shown a good prediction of the fatigue life.

The aim of this paper is to revaluate the SF method which is not easy to apply due to the difficulty in the estimate of the characteristic length of the material [19]. This reassessment relies on finding a relationship between the critical distance *L* and the characteristic length $\rho^*$ used in the support factor formula given by Siebel [8] and expanded by Neuber [9]. This approach aims to transfer all the data available in the literature for the critical distance *L* to the calculation of $\rho^*$, for which scanty and uncertain data exist. Moreover, the procedure to assess the critical distance *L* is clearly defined in the technical literature; hence it can be applied also to new materials. The motivation of the work is that the classic local gradient approach could still represent a reliable alternative to the TCD in the prediction of the fatigue life of machine components, gone out of fashion mainly due to the scarce information about $\rho^*$. In particular, it is highlighted that the SF method relies simply on the knowledge of the stress value and its gradient at the hot spot. By contrast, the TCD needs to know the stress distribution for a finite length inside the component. Therefore, the SF method requires less information and leads to simpler computational procedures to gather the needed data than the TCD.

The work is organized as follows. First, given a plausible stress gradient curve, the analytical relationship between the critical distance *L* and the characteristic length $\rho^*$ is retrieved. The underlying hypothesis of the same fatigue life prediction between the two methods, thus meaning the same effective stress is forced in the stress curve adopted. Second, by relying on this analytical relationship, the methods are compared, taking the Taylor's one as reference on three different benchmark geometries. First, it is analyzed an open V-notch deeply discussed in [20]. Second, the stress state in a thick walled vessel is considered. Third, the fatigue life of a real application of a complex oleo-hydraulic distributor under internal pressure, provided by Galtech Srl, is estimated.

In the first two cases, being available a closed form analytical solution for the stress field, a systematic comparison was performed. In the first case there is a difference between TCD and SF effective stress, while in the second one the two methods produce a similar prediction. In the third case, two critical hot spots were investigated and the methods produce almost the same prediction for the first hot spot while the difference in terms of effective stress for the second one is lower than 30%.

## 2. Materials and Methods

### *2.1. Support factor method*

The support factor (SF) method, considering for instance the formulation of Siebel [4], can be summarized in the following procedure. From the linear elastic stress analysis, the stress gradient $G_\sigma$ is calculated as:

$$G_\sigma = \left.\frac{d\sigma}{dx}\right|_{x=0} \tag{2}$$

being $\sigma$ the elastic stress (equivalent or principal stress) at the hot spot (Figure 1), and $x$ the coordinate axis starting at the hot spot and normal to the surface. The ratio between the stress gradient $G_\sigma$ and the maximum stress $\sigma_{max}$ gives the normalized stress ratio as:

$$s_\sigma = \frac{G_\sigma}{\sigma_{\max}} \tag{3}$$

Hence, the support factor $v_d$ is calculated as:

$$v_d = 1 + \sqrt{\rho^* \cdot s_\sigma} \tag{4}$$

where $\rho^*$ is the characteristic length, a material constant which was seen as an indicator of the sliding layer of the plastic deformation by Siebel [8] or as a substitution internal notch radius by Peterson [7]. A common finding is that $\rho^*$ depends on the chemical composition, the technological process and the microstructure of the material [2] which can be evaluated through experimental tests on the material.

The SF method calculates the effective stress $\sigma_{eff}^S$ to be used in the S-N curve as:

$$\sigma_{eff}^S = \frac{\sigma_{\max}}{v_d} \tag{5}$$

### *2.2. Theory of Critical Distance*

Similarly to the SF method, the TCD proposed by Tanaka and Taylor [1-2] relies on a linear elastic stress analysis to calculate the stress field in the component. Once the peak elastic stress $\sigma_{max}$ is identified, the effective stress $\sigma_{eff}^T$ is calculated as the stress value occurring at a critical distance $L$ from the peak stress, along the same direction as in the SF method. Among the several proposals found in literature, the critical distance $L$ is here calculated using El Haddad's equation [16]:

$$L = \frac{1}{\pi}\left(\frac{\Delta K_{th}}{S'_n}\right)^2 \tag{6}$$

where $\Delta K_{th}$ is the threshold stress intensity factor, and $S'_n$, the fatigue limit for a smooth specimen. This critical distance corresponds to the maximum acceptable length of an equivalent defect or crack that does not undergo propagation. Values of critical distance are in the range from 50 μm for some high strength steels to near 4 mm for gray cast iron. Once the critical distance is found the effective stress is calculated from the principal stress distribution as shown in Fig. 1.

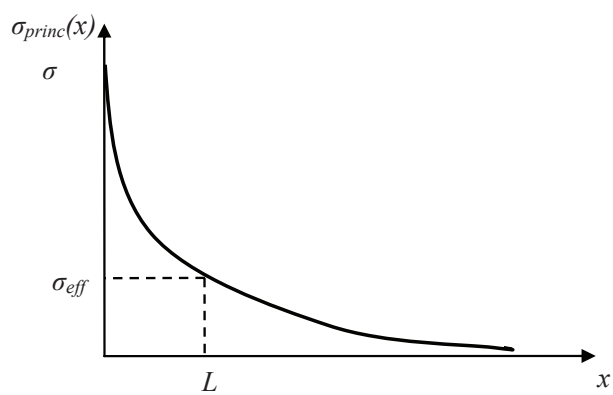


Fig. 1. Typical stress distribution along the direction normal to the surface

### 2.3. Material parameter correlation

The idea proposed in this paper is to correlate the characteristic length $\rho^*$ of the SF method (section 2.1) with the critical distance $L$ of the TCD (section 2.2). In order to find a correlation, an analytical test curve for the stress distribution is built. The function must comply with the following three constraints. First, the maximum stress $\sigma_{max}$ occurs at $x = 0$ in accordance with the typical stress distribution provided by notches. Second, at $x = 0$ the stress gradient is known. Third, the stress monotonically goes to a fraction of the maximum stress $\sigma_{max}$ as $x$ tends to infinite, as typically occurs, for example, for elastic plane with a hole under uniform tension. The simpler curve which complies with the above constraints is the homographic function, which can be generally written as:

$$\sigma(x) = \frac{Ax + B}{x + C} \tag{7}$$

The three constants $A$, $B$ and $C$ can be easily calculated by applying the above constraints:

$$\sigma(0) = \sigma_{\max} \qquad \left.\frac{d\sigma}{dx}\right|_{x=0} = G_\sigma \qquad \lim_{x\to\infty} \sigma(x) = k\sigma_{\max} \tag{8}$$

By solving the relationships *(8)* the unknown constants are calculated and yield the following expression of the homographic function:

$$\sigma(x) = \sigma_{\max} \frac{kxs_\sigma - k + 1}{xs_\sigma - k + 1} \tag{9}$$

It is possible to apply the TCD to the stress function *(9)* and hence the effective stress according to the TCD is obtained:

$$\sigma_{eff}^T = \sigma(L) \tag{10}$$

Enforcing the equivalence of the two methods means to have the same cycles to failure:

$$N^S = N^T \tag{11}$$

and considering an arbitrary material with a certain Wohler curve implies the equality of the effective stresses given by the two methods.

$$\sigma_{eff}^S = \sigma_{eff}^T = \sigma_{eff} \tag{12}$$

This leads to the following relationship between the material parameters $L$ and $\rho^*$.

$$\rho^* = \frac{Ls_\sigma (1-k)^2}{(Lks_\sigma - k + 1)^2} L \tag{13}$$

Equation (13) represents the link between $\rho^*$ and $L$, obtained for the stress distribution given in *(9)* and can be applied to any geometry in order to compare the prediction of the two methods. Finally, the following expression is obtained for the support factor $\nu_d$:

$$\nu_d = \frac{Ls_\sigma - k + 1}{Lks_\sigma - k + 1} \tag{14}$$

The general expression given by equation (13) and (14) for $\rho^*$ and $\nu_d$ respectively, are dependent on the parameter $k$, which is defined in the third of (8). Even though the value of this parameter is arbitrary, as a general rule it can be assumed that the stress falls to zero at infinite, thus leading to $k = 0$. This condition is analitically true for example in case of a vessel under internal pressure. Hence, the following simplified formuas are obtained for $\rho^*$ and $\nu_d$ respectively:

$$\rho^* = L^2 s_\sigma \tag{15}$$

$$\nu_d = L s_\sigma + 1 \tag{16}$$

Using the above design formulas it is possibile to sum up the values of $\rho^*$ (Table 1) and $\nu_d$ (Table 2) as function only of the critical distance $L$ and the normalized stress gradient $s_\sigma$ . In particular, the support factor $\nu_d$ gives an immediate information to the designer about the fatigue life prediction of the component based simply on three parameters: maximum elastic stress, stress gradient at the hot spot and critical distance of the material.

## 3. Results and Discussion

Three benchmark geometries were considered in this section, in order to assess the proposed procedure for applying the SF method. The first and second one were two problems retrieved from literature and having an analytical solution, so direct relationships can be found between the geometric parameters and the critical distance of the material. The last one was an industrial problem of a complex oleo-hydraulic distributor under internal pressure, where the maximum principal stress field was derived by a finite element analysis.

### *3.1. Open V-notch in a plate*

Fig. 2a shows the first benchmark geometry, a general open notch with tip radius in a plate, deeply analyzed by Lazzarin et al [20].

The general expression for the stress in mode I calculated along the principal direction is found to be:

$$\sigma_\theta\big|_{\theta=0} = \sigma_{\max}\left(\frac{r}{r_0}\right)^{\lambda_1-1} \frac{(1+\lambda_1)+\chi_{b1}(1-\lambda_1)+\{p/4(p-1)\}(r/r_0)^{\mu_1-\lambda_1}\left[\chi_{d1}(1+\mu_1)+\chi_{c1}\right]}{(1+\lambda_1)+\chi_{b1}(1-\lambda_1)+\{p/4(p-1)\}\left[\chi_{d1}(1+\mu_1)+\chi_{c1}\right]} \tag{17}$$

where $r_0$ represents the tip radius of the V-notch $r$ is the radial coordinate starting from the root of the notch and $p$ is a non dimensional group given by

$$p = \frac{2\pi - 2\beta}{\pi} \tag{18}$$

The other parameters in the equation are constants which depend only on the opening angle $\beta$ and are deeply described and provided in [20]. Although this equation is valid only in stress concentration regions and for notches in wide plates (theoretically the width and the notch depth can be regarded as infinite), the accuracy of the equation remains good along the axis of symmetry also for plates of finite width.

Since a closed form solution for the stress distribution is available *(17)*, the effective stress can be calculated both according to the TCD (section 2.2) and according to the SF method through the support factor of equation (16) . In particular, relationship (17) is assumed in order to define the critical length $\rho^*$ as a function of the critical distance $L$. For the sake of brevity the analytical calculation are not reported here.

Table 1. Characteristic length $\rho^*$

| $\rho^*$ | | Normalized stress gradient $s_\sigma$ (mm$^{-1}$) | | | | | | | | | | |
|---|---|---|---|---|---|---|---|---|---|---|---|---|
| | | **0.1** | **0.2** | **0.3** | **0.4** | **0.5** | **0.6** | **0.7** | **0.8** | **0.9** | **1** | **1.5** |
| Taylor critical distance $L$ (mm) | **0.1** | 0.001 | 0.004 | 0.009 | 0.016 | 0.025 | 0.036 | 0.049 | 0.064 | 0.081 | 0.100 | 0.225 |
| | **0.25** | 0.003 | 0.010 | 0.023 | 0.040 | 0.063 | 0.090 | 0.123 | 0.160 | 0.203 | 0.250 | 0.563 |
| | **0.5** | 0.005 | 0.020 | 0.045 | 0.080 | 0.125 | 0.180 | 0.245 | 0.320 | 0.405 | 0.500 | 1.125 |
| | **0.75** | 0.008 | 0.030 | 0.068 | 0.120 | 0.188 | 0.270 | 0.368 | 0.480 | 0.608 | 0.750 | 1.688 |
| | **1** | 0.010 | 0.040 | 0.090 | 0.160 | 0.250 | 0.360 | 0.490 | 0.640 | 0.810 | 1.000 | 2.250 |
| | **1.25** | 0.013 | 0.050 | 0.113 | 0.200 | 0.313 | 0.450 | 0.613 | 0.800 | 1.013 | 1.250 | 2.813 |
| | **1.5** | 0.015 | 0.060 | 0.135 | 0.240 | 0.375 | 0.540 | 0.735 | 0.960 | 1.215 | 1.500 | 3.375 |
| | **1.75** | 0.018 | 0.070 | 0.158 | 0.280 | 0.438 | 0.630 | 0.858 | 1.120 | 1.418 | 1.750 | 3.938 |
| | **2** | 0.020 | 0.080 | 0.180 | 0.320 | 0.500 | 0.720 | 0.980 | 1.280 | 1.620 | 2.000 | 4.500 |
| | **2.25** | 0.023 | 0.090 | 0.203 | 0.360 | 0.563 | 0.810 | 1.103 | 1.440 | 1.823 | 2.250 | 5.063 |
| | **2.5** | 0.025 | 0.100 | 0.225 | 0.400 | 0.625 | 0.900 | 1.225 | 1.600 | 2.025 | 2.500 | 5.625 |
| | **2.75** | 0.028 | 0.110 | 0.248 | 0.440 | 0.688 | 0.990 | 1.348 | 1.760 | 2.228 | 2.750 | 6.188 |
| | **3** | 0.030 | 0.120 | 0.270 | 0.480 | 0.750 | 1.080 | 1.470 | 1.920 | 2.430 | 3.000 | 6.750 |
| | **3.25** | 0.033 | 0.130 | 0.293 | 0.520 | 0.813 | 1.170 | 1.593 | 2.080 | 2.633 | 3.250 | 7.313 |
| | **3.5** | 0.035 | 0.140 | 0.315 | 0.560 | 0.875 | 1.260 | 1.715 | 2.240 | 2.835 | 3.500 | 7.875 |

Table 2. Support factor $\nu_d$

| $\nu_d$ | | Normalized stress gradient $s_\sigma$ (mm$^{-1}$) | | | | | | | | | | |
|---|---|---|---|---|---|---|---|---|---|---|---|---|
| | | **0.1** | **0.2** | **0.3** | **0.4** | **0.5** | **0.6** | **0.7** | **0.8** | **0.9** | **1** | **1.5** |
| Taylor critical distance L (mm) | **0.1** | 1.010 | 1.020 | 1.030 | 1.040 | 1.050 | 1.060 | 1.070 | 1.080 | 1.090 | 1.100 | 1.150 |
| | **0.25** | 1.025 | 1.050 | 1.075 | 1.100 | 1.125 | 1.150 | 1.175 | 1.200 | 1.225 | 1.250 | 1.375 |
| | **0.5** | 1.050 | 1.100 | 1.150 | 1.200 | 1.250 | 1.300 | 1.350 | 1.400 | 1.450 | 1.500 | 1.750 |
| | **0.75** | 1.075 | 1.150 | 1.225 | 1.300 | 1.375 | 1.450 | 1.525 | 1.600 | 1.675 | 1.750 | 2.125 |
| | **1** | 1.100 | 1.200 | 1.300 | 1.400 | 1.500 | 1.600 | 1.700 | 1.800 | 1.900 | 2.000 | 2.500 |
| | **1.25** | 1.125 | 1.250 | 1.375 | 1.500 | 1.625 | 1.750 | 1.875 | 2.000 | 2.125 | 2.250 | 2.875 |
| | **1.5** | 1.150 | 1.300 | 1.450 | 1.600 | 1.750 | 1.900 | 2.050 | 2.200 | 2.350 | 2.500 | 3.250 |
| | **1.75** | 1.175 | 1.350 | 1.525 | 1.700 | 1.875 | 2.050 | 2.225 | 2.400 | 2.575 | 2.750 | 3.625 |
| | **2** | 1.200 | 1.400 | 1.600 | 1.800 | 2.000 | 2.200 | 2.400 | 2.600 | 2.800 | 3.000 | 4.000 |
| | **2.25** | 1.225 | 1.450 | 1.675 | 1.900 | 2.125 | 2.350 | 2.575 | 2.800 | 3.025 | 3.250 | 4.375 |
| | **2.5** | 1.250 | 1.500 | 1.750 | 2.000 | 2.250 | 2.500 | 2.750 | 3.000 | 3.250 | 3.500 | 4.750 |
| | **2.75** | 1.275 | 1.550 | 1.825 | 2.100 | 2.375 | 2.650 | 2.925 | 3.200 | 3.475 | 3.750 | 5.125 |
| | **3** | 1.300 | 1.600 | 1.900 | 2.200 | 2.500 | 2.800 | 3.100 | 3.400 | 3.700 | 4.000 | 5.500 |
| | **3.25** | 1.325 | 1.650 | 1.975 | 2.300 | 2.625 | 2.950 | 3.275 | 3.600 | 3.925 | 4.250 | 5.875 |
| | **3.5** | 1.350 | 1.700 | 2.050 | 2.400 | 2.750 | 3.100 | 3.450 | 3.800 | 4.150 | 4.500 | 6.250 |

Fig. 3 compares the effective stresses from both methods as a function of the ratio between $L$ and $r_0$ for three different values of the opening angle $\beta$. Both the curves of the effective stress are normalized over the maximum

stress $\sigma_{max}$ *(17)* in order to provide a more general comparison. It appears that the effective stress provided by the SF method is always lower than the one provided by the TCD, in particular as the ratio between the critical distance $L$ and the geometric dimension $r_0$ increases. A good agreement between the methods is obtained when the ratio $L/r_0$ is below 1, i.e. when the critical distance is comparable with the notch tip radius dimension. A difference up to 50% is registered as the ratio $L/r_0$ equals five, corresponding to sharp notches in conjunction with a material which is not much sensible to notches (like cast iron).

This significant difference as the critical length increases or the tip radius decreases is due to the assumption of $k = 0$ which make function (9) go to zero as $x$ tends to infinite. By contrast, this notched plate is under uniform tension and hence the stress cannot fall to zero.

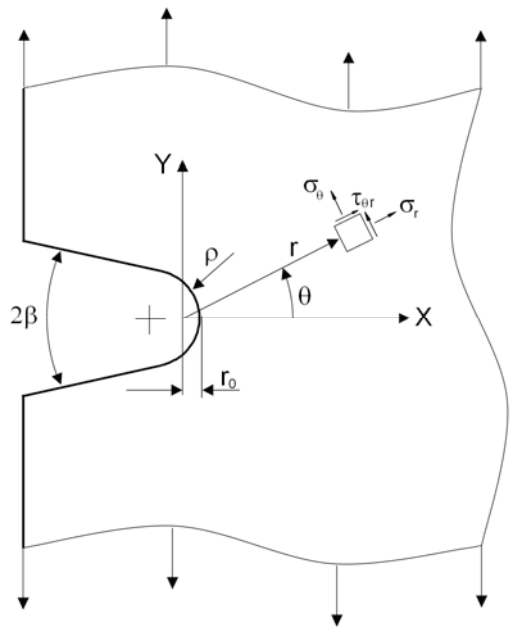


Fig. 2. Coordinates system used for the elastic analysis in [19]

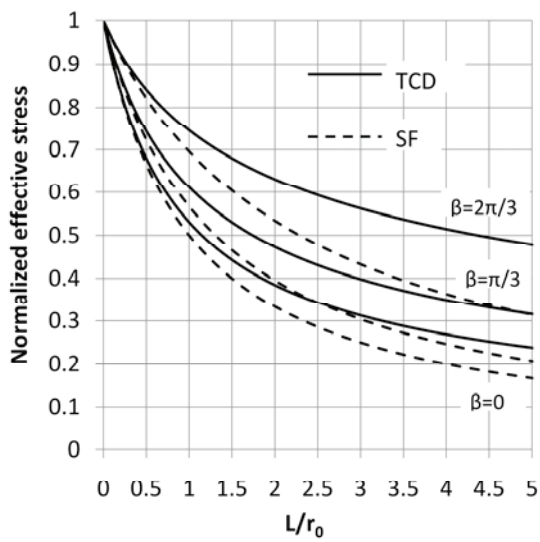


Fig. 3. Hoop effective stress calculated with TCD approach (solid line) and SF approach (dashed line) for three opening angles

### 3.2. Thick-walled vessels under internal pressure

The well known elastic problem of a thick walled vessel under pressure is used as a second benchmark. The solution of a thick vessel of internal radius $r_i$, external radius $r_e$ under internal pressure $p_i$ can be solved using the Lamè equations [21] for the radial stress $\sigma_r$:

$$\sigma_r = A + \frac{B}{r^2} \tag{19}$$

and for the hoop stress $\sigma_\theta$:

$$\sigma_\theta = A - \frac{B}{r^2} \tag{20}$$

where the constants $A$ and $B$ are determined from the boundary conditions.

Focusing on the hoop stress, its explicit expression considering the boundary conditions $p_i \neq 0$ and $p_e$=0 is:

$$\sigma_\theta = p_i \frac{r_i^2}{r_e^2 - r_i^2}\left(\frac{r_e}{r^2} + 1\right) \tag{21}$$

From this closed form solution for the principal stress distribution, the effective stress can be calculated both according to the TCD (section 2.2) and according to the SF method considering the support factor of equation (16). Fig. 4 compares the effective stresses from both methods as a function of the ratio between $L$ and $r_i$. The effective stress is normalized over the maximum effective stress obtained with the TCD method in order to give more a general comparison.

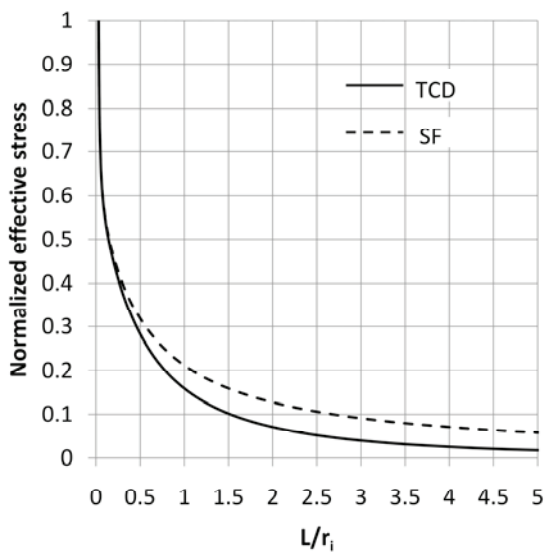


Fig. 4. Thick walled vessel under internal pressure. Comparison of TCD and SF effective stresses as a function of the ratio between critical distance $L$ and internal radius $r_i$

It appears that the effective stress provided by the SF method is higher than the one provided by the TCD, in particular as the ratio between the critical distance $L$ and the geometric dimension $r_i$ increases. However, the trend between the methods is the same, due to the peculiarity of the benchmark in which hoop stresses decrease to zero as the wall thickness increases. This is consistent with the assumption of $k$ = 0 adopted for the homographic function.

The non dimensional ratio $L/r_i$ gives an indication about the combined action of notches and type of material considered. High values of $L/r_i$ can be found with sharp notches or cracks combined with materials with low sensibility to the notches (like cast iron). On the contrary, low values of $L/r_i$ can be found with blunt notches and materials such as high strength steels, which exhibit very high sensitivity to notches.

### *3.3. Case study: hydraulic distributor*

Fig. 5a shows the third benchmark examined in this work: an industrial hydraulic multistage distributor taken from the fluid power industrial field, usually equipping off-highway vehicles and excavators. The valve body was produced by casting in a sand mold with an internal sand core to realize a complex channels system. During the manufacturing, some of the ducts were machined to achieve a very refined and smooth surface condition and thus the nominal geometry was really close to the real geometry. The material was a gray cast iron (GJL-300) commonly used in fluid power applications due to its very good forming and cost-effectiveness. This is a very challenging field for the design and the prediction of the fatigue life of a notched component, because they have to operate for very long lives, under very high internal pressure. The analysis is organized in two steps. First, a linear elastic FE analysis was performed on a section of the component since the geometry was too complex and no analytical approaches were applicable. Second, the fatigue life prediction provided by the TCD and SF method is compared in some critical points (called hot-spots).

The component under study is a part of more complex system obtained by stacking several of these valves body and tightening up with some tie rods (Fig. 5a). The linear elastic FE analysis was focused on a module of the hydraulic distributor, crossed by several internal channels distributing pressurized oil to the outlets.

Table 3 collects the material characteristics in terms of mechanical and fatigue behaviour as reported by Baicchi et al. [22]. The Wohler S/N curve of the material was approximated from the experimental results through the Basquin equation [23]:

$$\sigma_a = \sigma_f (N)^n \tag{22}$$

Table 3. Mechanical and fatigue properties of GJL-300 [17]

| $E$(GPa) | $R_s$ (MPa) | $R_m$ (MPa) | $\sigma_f$ (MPa) | $n$ | $S'_n$ (MPa) | $\Delta K_{th}$ (MPa m^1/2) | | $L$ (mm) |
|---|---|---|---|---|---|---|---|---|
| 109 | 200 | 230 | 695 | -0.814 | 101 | R = 0.1 | 8 | 2.4 |
| | | | | | | R = 0.5 | 5.7 | |

Since stress concentrations are sought, a very refined mesh was performed on the three-dimensional model. In particular, where the critical features like inner ducts, notches, changes of sections and channels intersections occurs the average size of the element was between 0.4 mm up to 0.2 mm (Fig. 5b). Linear tetrahedral elements were used and the material was described as linear elastic. This mesh refinement was obtained after a convergence procedure on the model. The boundary conditions applied reproduced both the force exerted by the tie rods and the symmetry plane which allow only one half of the body to be modelled. More specifically, assembly of the system constraints the external faces of the valve to remain plane. This was described through internal kinematic constraints on the nodes lying on the external faces. A pressure equal to 40 MPa was applied to the inner pressurized channels. The analysis was implemented using a commercial FE Software, ABAQUS 6.9 [24]. Approximate real dimensions of the cast are (175x160x60 mm).

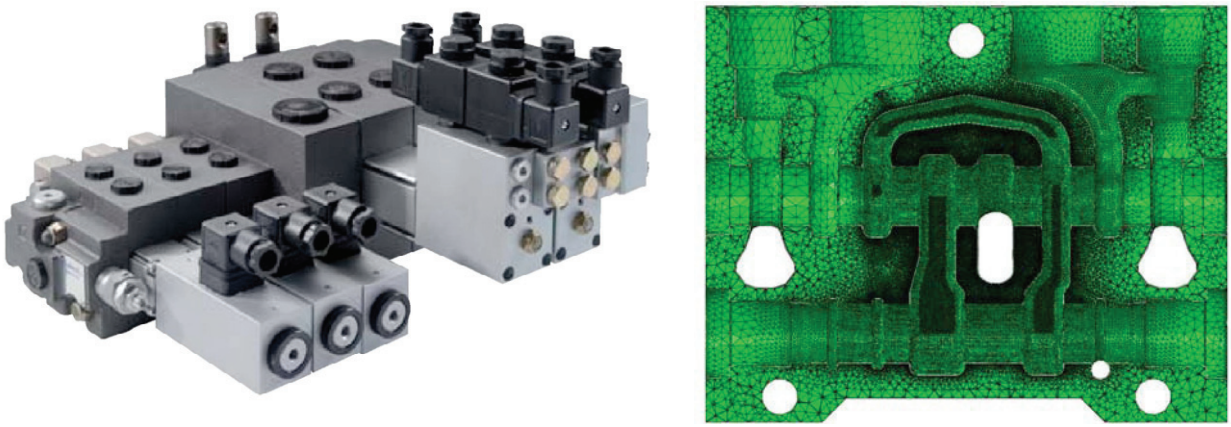

(a) (b)

Fig. 5. Modular architecture of the system (a), mesh of the model (b)

The analyses were performed on a workstation equipped with a quadcore processor i7 and 12 GB of RAM. Table 4 reports detailed information about the mesh and the model.

Fig. 6a shows the distribution of the maximum principal stress on the whole model while Fig. 6b focuses on the two most critical points (hot spots), which occur at the inlet channel of the distributor. The comparision between the two method for fatigue life prediction is thus performed in this two hot spots.

Table 4. Detailed mesh information

| Mesh type | Average element size | Elements | Nodes | D.o.F. |
|---|---|---|---|---|
| Refined | 0.3 | 4412982 | 8140252 | 2444589 |

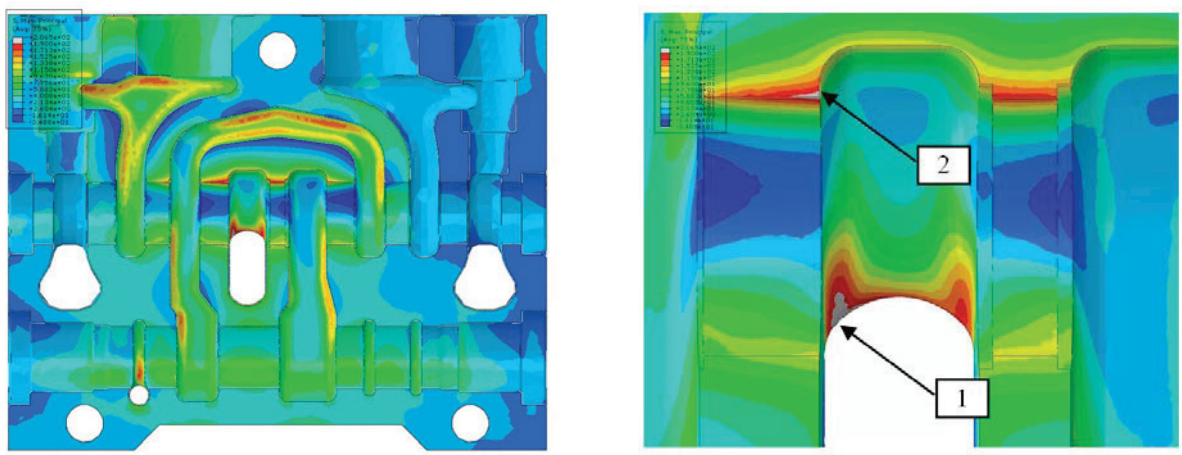


(a) (b)

Fig. 6. Maximum principal stresses on the valve body (a), and detail of the two critical hot spots (in gray) considered in the analysis (b).

Fig. 7 shows the distributions of the maximum principal stress (solid line), obtained through a subroutine specifically implemented, starting from the hot spots and extending inside the component along the maximum principal direction. These distributions were retrieved from the results of the FE model through an ad hoc computational procedure. In particular, Fig. 7a refers to the hot spot number 1 (Fig. 6b) while of Fig. 7b refers to the hot spot number 2 (Fig. 6b).

The TCD effective stress was calculated from Fig. 7 at the intersection of the critical distance of EN-GJL 300 ( Table 3) and represented with a dotted line. The SF effective stress was calculated, for both the hot spots, applying numerically the procedure of section 2.3 to the stress curves reported in Fig. 7. The characteristic length $\rho^*$ through of equation (15) is found equal to 3.88 mm and 4.96 mm respectively for the curve of Fig. 7a and b. This corresponds to an effective stress equal to 84.02 MPa and 108.01 MPa (dashed line) respectively.

It appears that with regard to the hot spot number 1 (Fig. 7a) the two methods provide exactly the same value of the effective stress. On the contrary, Fig. 7b highlights that for the hot spot number 2 the SF effective stress is lower than 29% than the TCD effective stress (119.3 MPa).

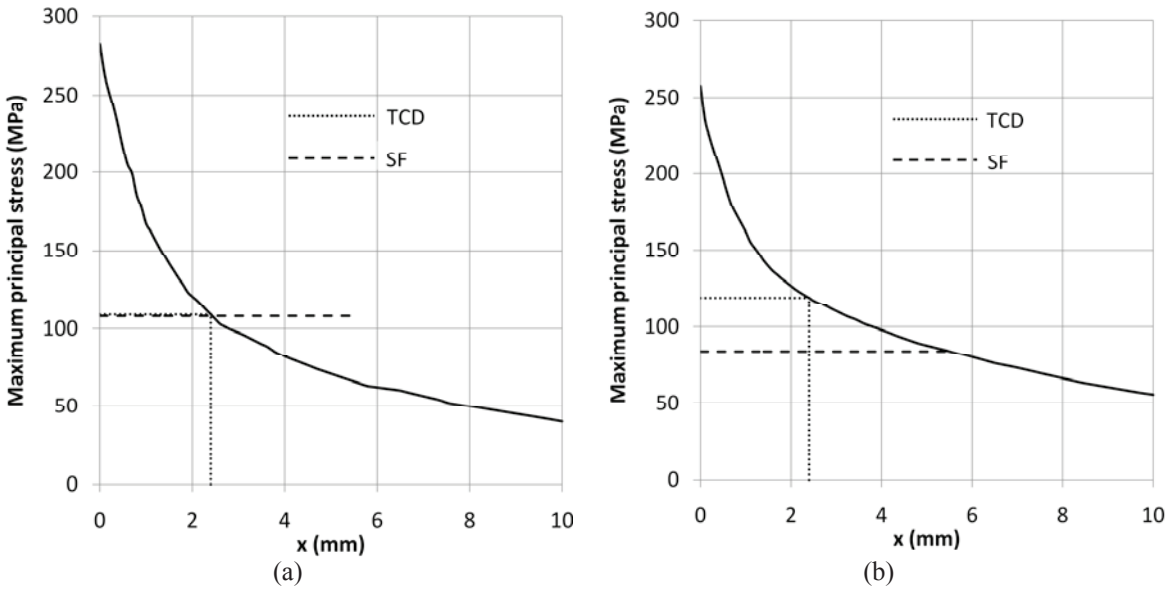


Fig. 7. Stress distribution at the hot spot 1 and correspondent effective stresses (a) and stress distribution at the hot spot 2 and correspondent effective stresses (b) calculated with both methods

## 4. Conclusions

Among the number of methods for fatigue life prediction of machine components the support factor method proposed by Siebel, Neuber and Peterson can still represent a reliable approach. A peculiarity of the method is that it relies only on the knowledge of the maximum stress and stress gradient in the hot spot. Its main drawback is the need of a material parameter $\rho^*$, which is known only for a few materials. A correlation between $\rho^*$ and the critical distance $L$ of the TCD is proposed in this paper. This correlation allow $\rho^*$ to be calculated for the same materials whose critical distance value is known. Relying on a specific stress function, the same fatigue life prediction between the SF method and the TCD is forced, obtaining a material parameter $\rho^*$ which depends only on critical distance $L$ and on local stress gradient $s_\sigma$. The proposed procedure is validated against two theoretical and one industrial benchmark. A systematic comparison is performed for a V-notch in a plate and a pressure vessel (first two benchmarks) showing a fair agreement between the methods over a wide range of ratios of critical length $L$ to a peculiar geometric dimension. Also in the case of the oleo-hydraulic distributor (third benchmark), where the comparison was focused on two hot spots given by an elastic finite element analysis, both the SF method and the TCD provide similar results.

## References

[1] K. Tanaka, Engineering formulae for fatigue strength reduction due to crack-like notches, *Int J Fract* 1983;**22**:R39–R45.

[2] D. Taylor, Geometrical effects in fatigue: a unifying theoretical model, *Int J Fatigue* 1999;**21:**413–20.

[3] Taylor D, Wang G. The validation of some methods of notch fatigue analysis. *Fatigue Fract Engng Mater Struct* 2000;**23**:387–94.

[4] Taylor D. Crack modelling: a technique for the fatigue design of components. *Engng Fail Anal* 1996;**3**(2):129–36.
[5] Taylor D, Hughes M, Allen D. Notch fatigue behaviour in cast irons explained using a fracture mechanics approach. *Int J Fatigue* 1996;**18**(7):439–45.
[6] Taylor D. The theory of critical distances: a new perspective in fracture mechanics. 1st ed.Oxford: Elsevier; 2007.
[7] Peterson RE. Notch sensitivity. In: Sines G, Waisman JL, editors. *Metal Fatigue*, New York: McGraw-Hill; 1959, p. 293–306.
[8] Siebel E, Stieler M. Dissimilar stress distributions and cyclic loading. *Z Ver Deutsch Ing* 1955;**97**:121–31.
[9] Neuber, H. Theory of Notch Stress: Principles for Exact Calculation of Strength with Reference to Structural form and Material. Springer Verlag, Berlin; 1958.
[10] Pilkey WD. Peterson's stress concentration factors. 2nd ed., New Jork: John Wiley & Sons; 1997.
[11] B. Reggiani and A. Freddi. Effetto supporto, tensione locale e gradiente relativo di tensione nella predizione della vita a fatica. *Frattura ed Integrità Strutturale* 2008;**4:**2–11.
[12] Heywood RB. The relationship between fatigue and stress concentration, *Aircraft Engineering* 1947;**19**:81-4
[13] Bollenrath F, Troost A. Wechselbeziehungen zwischen Spannungs-und Verformungsgradient. Teil 1. *Arch. Eisenhuttenwesen* 1950;**21**(11/12):431-6
[14] Bollenrath F, Troost A. Wechselbeziehungen zwischen Spannungs-und Verformungsgradient. Teil 2. *Arch. Eisenhuttenwesen* , 1951:**22**(9/10):327-35.
[15] Eichlseder W. Fatigue analysis by local stress concept based on finite elements results, *Computers and Structures* 2002:**80**:2109-13.
[16] Eichlseder W. Synthetic S/N curves. In: Topping BHV (editor). *Computational Techniques for Materials, Composites and Composite Structures*, Edinburgh: Civil-Comp Press; 2000, p. 161-4.
[17] Niemann G, Winter H, Hohn BR, Maschinenelemente, Springer; 2005.
[18] El Haddad MH et al. J integral applications for short fatigue cracks at notches. *Int J Fract* 1980;**16**:15–24.
[19] Taylor D, Bologna P, Bel Knani K. Prediction of fatigue failure location on a component using a critical distance method. *Int J Fatigue* 2000;**22**:735–42.
[20] Filippi S, Lazzarin P, Tovo R. Developments of some explicit formulas useful to describe elastic stress fields ahead of notches in plates. *Int J Sol Struct* 2002;**39**:4543-65.
[21] Timoshenko S, Goodier J. N., Theory of Elasticity, 2nd ed. McGraw-Hill; 1951.
[22] Baicchi P, Collini L, Riva E. A methodology for the fatigue design of notched castings in gray cast iron. *Engng Fract Mech* 2007;**74**:539–48.
[23] Dowling E. Mechanical behavior of materials. 3rd ed. Prentice-Hall; 2006.
[24] Simulia ABAQUS 6.9, “Users’ Manual”, HKS Inc., Providence, RI, USA, (2009).